Modeling the impact of river discharge and wind on the hypoxia off Yangtze Estuary

Jingjing Zheng[1,2], Shan Gao[1,3], Guimei Liu[1,3*], Hui Wang[1,3]

1. National Marine Environmental Forecasting Center, Beijing 100081, China
2. State Key Laboratory of Marine Environmental Science, Xiamen University, Xiamen 361005, China
3. Key Laboratory of Research on Marine Hazards Forecasting, National Marine Environmental Forecasting Center , Beijing 100081, China

Abstract: The phenomenon of low dissolved oxygen (known as hypoxia) in coastal ocean system is closely related to a combination of anthropogenic and natural factors. Marine hypoxic occurs in the Yangtze Estuary, China with high frequency and long persistence. It's known that it related primarily to organic and nutrient enrichment influenced by river discharges and physical factors, such as water mixing. In this paper, a three-dimensional hydrodynamic model was coupled to a biological model to simulate and analyze the ecological system of the East China Sea. By comparing with the observation data, the model results can reasonably capture the physical and biochemical dynamics of the Yangtze Estuary. In addition, the sensitive experiments were also used to examine the role of physical forcing (river discharge, wind speed, wind direction) in controlling hypoxia in waters adjacent to the Yangtze Estuary. The results showed that the wind field and river discharge have significant impact on the hypoxia off the Yangtze Estuary. The seasonal cycle of hypoxia was relatively insensitive to synoptic variability in the river discharge, but integrated hypoxic areas were sensitive to the whole magnitude of river discharge. Increasing the river discharge was shown to increase hypoxic areas, while decreasing the river discharge was tended to decrease hypoxic areas. And the variations of wind speed and direction had great impact on the seasonal variability of hypoxia and the integrated hypoxic areas.

Key word: Yangtze Estuary, wind, river discharge, hypoxia

Fundation item: The National Natural Science Foundation of China under contract No. 41222038, 41076011，41206023 ; from the National Basic Research Program of China ("973" Program) under contract No. 2011CB403606;and.the "Strategic Priority Research Program" of the Chinese Academy of Sciences Grant No. XDA1102010403.

*Corresponding author, E-mail: liugm@nmefc.gov.cn

1. Introduction

In recent decades, the eutrophication of water body driven by excess nutrient loads from lands due to human activities is increasing year by year, which leads to an enhancement of hypoxic zone (Murphy et al., 2011; Rabouille et al., 2008). Dissolved oxygen (DO) threatens marine animals when its concentration is lower than 2 mg/L or 62.5 umol/L, which is defined as hypoxia (Diaz, 2001; H Wei et al., 2007). When DO is less than 2.0 mg/L, the majority of marine aquatic organisms will be dead, especially benthic animal (Karlson et al., 2002). Hypoxia is one of the most severe environmental issues affecting estuarine and coastal marine ecosystems around the world. Hypoxia can reduce the diversity of marine species, change the community structure of marine organisms, reduce the richness of fish and benthic animals, and thus affect the fishery production and bring about direct or indirect economic loss (Yin et al., 2004).

The hypoxia off Yangtze Estuary was first found in 1959 (Gu, 1980). In recent years, with the increase of global warming and pollutant emissions, the hypoxic area off Yangtze Estuary expanded fast and became one of world's largest costal hypoxia (Vaquer-Sunyer and Duarte, 2008). In the 1950s, the occurrence probability on hypoxia off Yangtze Estuary in summer was 60%, while after 1990s hypoxia occurrence probability reached 90%, and hypoxic areas which were greater than 5000 km^2 basically occurred after the end of 1990s (Wang, 2009).

The formation of hypoxia adjacent to the Yangtze Estuary is a complex process, which is the result of both physical and biochemical processes. Previous research had shown that the formation and evolution of hypoxia were closely related to river discharge, Taiwan Warm Current, wind speed, wind direction, bottom topography, and the degradation of organic (Li et al., 2011; Ning et al., 2011; Wang, 2009; X Li, 2011; Zhou F, 2010; Zhu et al., 2011). It was generally accepted that the increase in hypoxic extent was mainly driven by the rising anthropogenic nutrient inputs from the Yangtze River. However many studies had indicated that the physical factors have important contributions to the formation of the annual variation of hypoxia. Wilson et al. (2008) found that the wind-driven circulation had an important influence on the West Long Island Strait stratification and vertical mixing. When the wind direction changed in summer, it prevented the exchange of dissolved oxygen from the bottom to surface, which made the West Long Island Strait appear hypoxia. Through numerical simulation, Obenour (2015) found that the river nutrient concentration was very important for the formation of hypoxia. However the stratification, which presented as a function of river discharge, wind speed and wind direction, contributed to a larger extent to the interannual variability in hypoxia. Due to the limitation of observation data, it was difficult to fully understand the temporal and spatial variation of hypoxia, and quantitatively described the influence of physical factors on the hypoxia off the Yangtze Estuary. In this paper, a three-dimensional

hydrodynamic model (Regional Ocean Model System, ROMS) coupled nitrogen cycle model described by Fennel et al. (2006) were used to simulate ecosystem of the East China Sea. Through this coupled model, the effects of river discharge, wind speed and wind direction on dissolved oxygen at sublayer and bottom of sea waters off the Yangtze Estuary were analyzed quantitatively.

2. Model description

2.1 Physical model

The physical circulation model used in this study was based on the Regional Ocean Model System, which was a free-surface, terrain-following, primitive equations ocean model (Haidvogel et al., 2008; Shchepetkin A F, 2005). This model was built for the East China Sea (114-143^{o}E, 22.3-53.1^{o}N) with a 1/15 degree horizontal resolution and 30 vertical layers (Fig. 1a). The models' terrain-following vertical layers were stretched to result in increased resolution near the surface and bottom. A fourth-order horizontal advection scheme for tracers, a third-order mixing by Mellor and Yamad were used in the model (Mellor G 1982). At the offshore open boundary, we employed Chapman's condition for surface elevation (Chapman, 1985), Flather's condition for barotropic velocity (Flather, 1976), and a combination of radiation condition and nudging for tracers (Marchesiello et al., 2001).

The model was initialized with climatological temperature, salinity from the Generalized Digital Environment Model (GDEM). The south, north and east of the pattern were open boundary, and the west was closed boundary. On the open boundary, the average profile of temperature, salinity and sea level were derived from Simple Ocean Data Assimilation (SODA). The model was forced with net heat flux, fresh water flux, short wave radiation, wind stress and so on, which derived from NCEP/CFSR reanalysis. In the model, the runoff of the Yangtze River was determined by the month average discharge of the Datong station (Liu Xincheng, 2002).

2.2 Biological model

The biological module was based on the nitrogen cycle model described in the study by Fennel et al. (2006). The model included ten state variables: two species of dissolved inorganic nitrogen (nitrate, NO_3 and ammonium, NH_4), one phytoplankton group, one zooplankton group, chlorophyll-a, two species detritus representing large, fast-sinking particles and suspended, small particles, and oxygen, total inorganic carbon, alkalinity. The sources of dissolved oxygen in the model were air–sea gas exchange, primary production, and the sink included the respiration zooplankton, nitrification, decomposing detritus and sediment oxygen consumption(Fennel et al., 2013). At the sediment-water interface, the model assumed "instantaneous remineralization" by which organic

matter that sank to the bottom was remineralized immediately to ammonium and oxygen was taken up immediately as well. The initial fields and boundary conditions for the biological tracers were derived from the World Ocean Atlas 2009 (WOA2009). The initial value of ammonium was set to 1mmol/m^3.The chlorophyll-a concentration was extrapolated in the vertical direction from surface values specified by SeaWiFS monthly climatological data and the extrapolation was based on the generalized Gaussian curve of typical pigment profile (Lewis et al., 1983; Morel and Berthon, 1989). The initial values of phytoplankton, zooplankton and detritus concentrations were set to 0.5, 0.25 and 0.25 times of chlorophyll-a concentration, respectively. Ammonium can be rapidly nitrified into nitrate at the inner estuaries. Therefore, only nitrate discharged from the Yangtze River was considered in the model.

After the physical model had spun-up for 10 year since climatological 1st January, the coupled physical-biological model was simulated from 1st January 2006 to 31th December 2011~~0~~. A series of numerical experiments in 2010 were set up to study the influence of river discharge, wind speed and wind direction on hypoxia adjacent to the Yangtze Estuary.

3. Results

3.1. Model validation

The model results and some observational data in the East China Sea were available to validate the model. These include monthly climatological values for SST and SSS with 1/4° spatial resolution from the GDEM, sea surface chlorophyll with a spatial resolution of 4 km from the MODISA in August 2011, and in situ biochemical data obtained from summer cruise in August 2011. Fig.1c showed the cruise observations along the section E with blue dots and sampling stations with red dots.

The comparison of sea surface temperature (SST) and sea surface salinity (SSS) in August between model and GDEM were shown in Fig. 2. The model fields of SST, SSS were~~are~~ the monthly mean climatological simulation for 10 years. And the GDEM fields are the monthly mean climatology data. The SST and SSS comparison shows the model performance was similar with the GDEM. The root mean square error (RMSE) of SST and SSS are approximately 1.18, 0.86 for model . ~~Apparently, the model results of SST and SSS were similar to GDEM data.~~ The spatial distribution characteristic of SST was gradually increasing from north to south. The model results of the SST along the coastal waters were higher than GDEM data, especially offshore of Bohai and the Yellow Sea. In August, under the control of southerly wind, the Yangtze diluted water expanded to the northeast direction. From the difference of SSS between simulated results and GDEM data, we found that a certain deviation between them near the Yangtze Estuary. In reality, the GDEM data was not very accurate along the China coast, due to its low spatial resolution. The distributions of SSS in our model were comparable to the results conducted by Liu et al. (2010).

Fig. 3a,3b showed that the comparison of sea surface chlorophyll-a concentration between the model results and MODISA~~SeaWiFS~~-derived data in August 2011. With regard to the chlorophyll-a, the RMSE was 1.31. It can

带格式的：段落间距段前：0.5 行，段后：0.5 行

带格式的：上标

带格式的：行距：单倍行距

be seen that the patterns of chlorophyll-a were comparable to the MODISA~~SeaWiFS~~-derived data. For example, the distribution of chlorophyll-a was extended to northeast in summer. The chlorophyll-a concentration was 5-10 mg/m^3 in surface waters adjacent to the Changjiang Estuary, then decreased rapidly eastward to the open shelf, where values were 0.1–0.5 mg/m^3. The modeled chlorophyll-a values in the inner and mid shelves were quite close to the MODISA~~SeaWiFS~~-derived data, while the model generally underestimated the chlorophyll-a in the outer shelf. Compared with the MODISA~~SeaWiFS~~-derived data, the concentration of chlorophyll in the south of 28^{o}N was also lower. This was mainly due to only consider the nutrient inputs form the Yangtze River in the model.

In-situ nitrate and ammonium distributions along section 30^{o}N (see Fig. 3) in August 2011 were used to evaluate the simulation capability of biological model. Both in-situ and model nitrate distributions showed that the presence of relative high nitrate in the bottom (>4 mmol/m3), but low (< 2 mmol/m3) in the surface. An analogous structure was present in the in-situ temperature and salinity distributions located between 123^{o}E and 124^{o}E reported by Wang (2009), so that upwelled water inside the trough involved not only low temperature and high salinity but also high nutrients. Form the Fig. 3c,3d, a definite deviation between the model and in situ data can be seen. The high nitrate concentration appeared above water layers of 25 meter along the section of 123^{o}E, but the model failed to reproduce it. The underestimation probably resulted from the insufficient dispersion of high nitrate, which was source from Yangtze river diluted water. Along the section of 30^{o}N, the patterns of model ammonium resembled that of observations. Ammonium was relatively high in the near-shore waters (>2 mmol/3), then decreased toward the open waters (<1 mmol/m3). An obvious high-concentration area was located between 123^{o}E and 124^{o}E, which reconfirmed that the Taiwan warm upwelling brought the bottom water with high nutrients to the surface.

Fig. 4 showed the comparison between in-situ and model results of dissolved oxygen and nitrate concentration at the stations in August 2011 (see Fig.1c). It can be seen that the simulated dissolved oxygen and nitrate resembled the in-situ data. The ~~root-mean-square error of~~ RMSE on surface dissolved oxygen, bottom dissolved oxygen, surface nitrate and bottom nitrate were 0.55, 0.56, 1.58 and 1.94 respectively. The mean bias (Mb) was defined as the difference between average values of models and observations. The Mb of surface dissolved oxygen and bottom dissolved oxygen were -0.31 mmol/m^3, 0.1mmol/m^3 respectively, which were acceptable. With regard to the bottom nitrate, Mb=0.79 mmol/m^3 indicated the model overestimates the bottom nitrate in average, while the surface nitrate performed much better with Mb=-0.1 mmol/m^3. The concentration of dissolved oxygen in the surface layer was generally high (>6 mg/L), while was low in the bottom. ~~The difference of nitrate concentration between the model results and in-situ data was relatively obvious. The reason may be that the river input of nitrate was monthly average in the model.~~

The distribution of dissolved oxygen adjacent to the Yangtze Estuary in September 2010 was showed in Fig.5. On the whole, it presented that the distribution of dissolved oxygen was high in the north and low in the south. A

带格式的：上标
带格式的：上标
带格式的：上标
带格式的：上标

closed area with oxygen level less than 2.0 mg/L was appeared off Yangtze Estuary, and was extended along the Yangtze Estuary to the Zhejiang coastal water. ~~The model results of dissolved oxygen were similar to that observed by Liu (2012).~~

3.2 The impacts of river discharge on hypoxia

To evaluate the role of the seasonal variation in river discharge on the hypoxic area, we conducted a sensitivity experiment (denoted as 'Qconst') where river discharge was set to the annual mean value for 2010 and the other conditions were the same as the Base model run (Table 1). The extent of hypoxic water off the Yangtze Estuary can be quantified by calculating the total area of water that has bottom dissolved oxygen concentrations below different threshold value (1.0 mg/L, 2.0 mg/L, 3.0 mg/L). If there was no special note, the hypoxic area was denoted as the area of DO<2 mg/L in this paper. In the Base model run, hypoxia zone was first appeared off the Yangtze Estuary in August~~July~~, then reached its peak in ~~August and~~ September, finally it was reduced and gradually disappeared in October (Fig.6a). The results were consistent with the findings of previous work conducted by Wei (2015). As shown in Fig. 6a, the seasonal variations in hypoxic area in the Qconst run were almost consistent with the Base model run, which suggested that the seasonal variation of hypoxic area was not remarkably affected by the temporal variation of the river discharge of Yangtze River. In addition, the area of the bottom dissolved oxygen concentration less than 1 mg/L, 2 mg/L and 3 mg/L decreased by 32%, 46%, 19% (Table 2) in the Qconst run. Next, to evaluate the role of magnitude of river discharge, we conducted Q2 and Q0.5 sensitivity experiments where the temporal variation in river discharge was preserved but the magnitude was doubled or halved, respectively for 2010. Doubling the river discharge increased nearly 7 times of the area where the bottom dissolved oxygen concentration was below the minimum threshold (1 mg/L). A reduction in the river discharge by 50% decreased the total integrated hypoxic area by 20% to nearly 63% under different threshold values.

Water stratification prevented the vertical exchange of dissolved oxygen, and it was an essential condition for the formation of hypoxia. In this paper, Frequency Brunt-Vaisala (N^2) was calculated to quantify the stratification strength, and it was denoted as the stratification strength between the surface and bottom water (Goni et al., 2006). The greater the N^2, the stronger stratification of the water was. The calculating area of N^2 was showed in Fig. 1c of the red rectangle. N^2 was calculated for 2010 in the all model runs.

$$N^2 = -\frac{g}{\rho}\frac{\partial \rho}{\partial z}$$

As shown in Fig. 6b, the stratification of water adjacent to the Yangtze Estuary had a significant relationship with the river discharge. Doubling the river discharge increased markedly the stratification strength, while reducing the discharge to 50% of the Base model run led to a significant decrease in the stratification. Fig. 7 showed the

带格式的：定义网格后自动调整右缩进，调整中文与西文文字的间距，调整中文与数字的间距

带格式的：上标

correlation of concentration between the bottom dissolved oxygen and the N^2. We could found that N^2 was inversely proportional to the concentration of bottom dissolved oxygen. The stronger the stratification, the lower concentration of bottom dissolved oxygen. The absolute values of correlation coefficient were higher than 0.6. The maximum of absolute correlation coefficient was 0.73 in the Q2 run, while the minimum in the Qconst run was 0.6. And the absolute correlation coefficient was 0.67, 0.64 respectively in the Base and Q0.5 run. ~~, and the maximum of absolute correlation coefficient was 0.73 in the Q2 run.~~

3.3 The impacts of wind forcing on hypoxia

The wind forcing also had a significant effect on the occurrence and development of hypoxia. Increasing wind speed enhanced the vertical mixing of water, and promoted the vertical exchange of dissolved oxygen, which would lead to break the formation of hypoxia (Scully, 2010b). The Yangtze Estuary is mainly controlled by the East Asian monsoon. The wind speed and wind direction have obvious seasonal variability over the Yangtze Estuary, namely low magnitude and dominantly southerly direction in summer (July to September) and relatively high magnitude and northerly direction in winter. In order to evaluate the role of seasonal changes in wind forcing, we conducted wind runs where the August wind (denoted as 'WAug') and January wind (denoted as 'WJan') was repeated each month of 2010, respectively. By forcing the model in this way, the winds had daily variations associated with the passage of weather systems, but the seasonal variation of speed and direction were removed. Although this kind of situation did not exist in practice, it was helpful for us to further understand the impacts of wind forcing on hypoxia. The seasonal variability of wind speed and direction had a great impact on the seasonal cycle of the simulated hypoxic area. When strong, northerly winds in January were repeated all year in the WJan run, the hypoxia off the Yangtze Estuary was nearly disappeared. In contrast, when in the WAug run where light, southerly wind conditions were repeated all year, the hypoxia was extensive from July to October (Fig. 8a), and the integrated hypoxic area (DO<2 mg/L) increased roughly 25% compared to the Base model run (Table 2). Hypoxic area also showed obvious seasonal changes. Hypoxic area was the largest in summer, while essentially no hypoxia was simulated in the other months. Possible reason was that the phytoplankton was affected by water temperature, and decreased in early spring and winter, so that the consumption of dissolved oxygen was reduced due to organic matter decomposition.

To further examine the effects of wind speed on the hypoxia, we conducted a 'W0.9' wind run where the wind speed decreased 10%, and a 'W1.1' wind run where the wind speed increased by 10% during the summer (July to September). The magnitude of summer wind speed had a significant impact on the hypoxic area off the Yangtze Estuary. When summer wind speed decreased, the integrated hypoxic area was increased by roughly 45%. While increasing in summer wind speed led to a reduction by nearly 64% of hypoxic area (Table 2).

Previous study had suggested that hypoxic area was also sensitive to wind direction (Scully, 2010a; Xia and Jiang, 2015). To further evaluate the influence of wind direction on the hypoxia, we conducted the model runs where summer wind direction (July to September) were systematically varied in the model forcing. As is typical in most summers, the wind during the 2010 summer is predominately from the south. In the wind direction sensitivity runs, the modeled wind forcing during the summer (July to September) was rotated by 180 °(W180 °), negative 90 °(W - 90 °), and positive 90 °(W + 90 °), resulting in model forcing had the summer winds from the north, east, and west, respectively (Table 1). Although these simulations were not realistic, they provide insights into the impacts of wind direction on the hypoxia. When the summer wind direction was from the north (W180^{o}), the integrated hypoxic area off Yangtze Estuary was the minimum, and reduced by nearly 30% compared with Base model run. The integrated hypoxic area was greatest when the summer wind came from the west (W + 90^{o}), and it was increased by nearly 20%. The summer wind direction from the east (W-90^{o}) led to a reduction by nearly 10% of the integrated hypoxic area (Table 2).

4. Discussion

4.1 Model validation

In Fig4, the difference of nitrate concentration between the model results and in-situ data was relatively obvious. The reason may be that the river input of nitrate was monthly average in the model. As shown in Fig5, hypoxia was present mainly in the southern and northern parts along the coast of the study area. The model results of hypoxia area were similar to that observed by Liu (2012). Model validation results showed that the model can reproduce the variations of biological variables and the hypoxia in summer at the bottom of the Yangtze Estuary in a certain extent. There were some deviations from the observed results in some areas, which could due to the complex biogeochemical cycle, parameterization, physical field and so on. At least, it's suggested that the model can capture some basic conditions of the key physical and biological processes in the Yangtze Estuary, which is helpful for further exploring the mechanism of the formation of hypoxia off the Yangtze Estuary.

4.~~2~~1 River discharge

Stratification was an important indicator of oxygen concentration in bottom water, which prevented the exchange of dissolved oxygen from the surface to bottom, eventually resulting in hypoxia in the bottom water (Rabouille et al., 2008). The simulated seasonal cycle of hypoxic area on the Qconst run was similar to the Base model run (Fig. 6a), which suggested that the temporal variation in river discharge was not an important factor controlling the seasonal cycle of hypoxic area. But the magnitude of Yangtze River discharge variation could lead

带格式的：字体：五号
带格式的：段落间距段前：0.5 行，段后：0.5 行
带格式的：字体：五号
带格式的：缩进：首行缩进： 2 字符，定义网格后自动调整右缩进，调整中文与西文文字的间距，调整中文与数字的间距
带格式的：字体：五号，非加粗

to significant changes on the hypoxic area. Increasing river discharge led to an expansion of the lighter, fresher river plume water offshore and an enhancement of stratification (Fig. 9a), which limited the effective supplement of surface high dissolved oxygen. This result consequently caused a reduction of bottom dissolved oxygen (Fig.9c). And the integrated hypoxic area was increased by 92%, the lowest value of bottom dissolved oxygen from the Base model run of 1.11 mg/L, reduced to 0.78 mg/L. Whereas decreasing river discharge reduced the stratification (Fig.9a), and thereby significantly increased the vertical oxygen flux through the pycnocline. As a result, the integrated hypoxic area decreased by 55% and the lowest value of bottom dissolved oxygen increased to 1.32 mg/L. This findings were consistent with the results of previous work conducted by Scully (2013). In addition, there was a significant negative correlation between the bottom dissolved oxygen and the stratification (Fig.7). When the water stratification was strong, the bottom dissolved oxygen was low. While the water stratification was weak, and the bottom dissolved oxygen was high. Fig. 9a further showed that doubling or halving the river discharge respectively enhanced or reduced stratification over the majority of the shelf in summer months, resulting in decrease or increase the bottom dissolved oxygen.

Increasing river discharge leaded to offshore extension of the fresher river plume water (Fig.10b), bringing rich nutrients to the eastward. As a result, surface chlorophyll over the majority of the eastern shelf was increased in Q2 run relative to the Base model run (Fig.9b), which caused the continuous decrease in oxygen level at the lower layer through decomposition of organic matters. In contrast, decreasing the river discharge confined the river plume water to near the river mouths (Fig.10c), which limited the nutrients to eastward. As seen in Fig 9b, surface chlorophyll was decreased over the majority of the shelf in Q0.5 run compared to the Base model run. Thus, bottom dissolved oxygen was increased and hypoxic zone was decreased, due to the decomposition of organic matters was reduced in the bottom water.

4.3~~2~~ Wind Forcing

Strong wind could trigger strong vertical mixing and promote the vertical exchange of dissolved oxygen, which broke the formation of hypoxia (Chen et al., 2014; Ni et al., 2014). Our simulated results showed that the variation in wind speed and direction significantly influence the stratification and hence the hypoxic area. In the WJan wind run, the strong wind homogenized the water column, reducing stratification and producing essentially no hypoxia throughout the year. Fig. 11a showed that N^2 was negative in the most areas, except in the eastern part of the Hangzhou bay, which suggested that the water mixing was strong and the vertical flux of dissolved oxygen increased in WJan wind run. As a result, the bottom dissolved oxygen concentration was increased (Fig. 11c), and there was almost no hypoxia in the bottom water off the Yangtze Estuary in WJan wind run. In addition, the strong northwest wind in January resulted in strong estuarine residual velocities that brought the high dissolved

oxygen from the north of Yellow Sea to Yangtze River Estuary. Therefore, even though the average stratification strength in WJan wind run was stronger than the Q0.5 run (Table 2), WJan nearly did not develop any hypoxia throughout the year. From the Fig.11b, it could be seen that the surface chlorophyll concentration of WJan wind run was significantly lower than the Base model run. The possible reason was that the strong wind from northwest in WJan wind run drove downwelling due to Ekman dynamics, which made the concentration of surface chlorophyll decreased, and ultimately led to an enhancement of dissolved oxygen through lower decomposition of organic matters. These finds were the same as the results reported in the study conducted in the northern Gulf of Mexico shelf by Feng (2014). Above all the reasons, in the WJan wind run there was almost no hypoxia in the summer adjacent the Yangtze River Estuary.

In contrast, in the WAug wind run, the persistently weak wind enhanced the stratification and reduced the vertical flux of dissolved oxygen, resulting in decreasing bottom dissolved oxygen and promoting widespread hypoxia. In addition, the concentration of surface chlorophyll was increased adjacent to Yangtze Estuary and along the coast of Zhejiang in the WAug wind run (Fig. 11b). This result suggested that bottom dissolved oxygen declined with the decomposition of organic matters.

Simulations of hypoxic area showed significant variability in the response to wind speed. In the W1.1 wind run, the increase in wind speeds was thought to play a key role in breaking down stratification and increasing the vertical flux of dissolved oxygen. Increased wind speeds generally raised bottom dissolved oxygen concentration (Fig. 11c). This finding was similar to the results conducted in the Louisiana Coasts, where the authors suggested that wind-induced vertical mixing could result in significant reductions in the hypoxic area (Wiseman et al., 1997). As shown in Fig. 11b, in the area of 28-32^{o}N 122-123.5^{o}E, decreased surface chlorophyll resulted in lower dissolved oxygen consumption, which increased the dissolved oxygen in the bottom water. In contrast, in the W0.9 wind run, the dissolved oxygen flux from the upper layers due to stronger stratification was reduced. And increased surface chlorophyll concentration on the north of 30^{o} led to huge dissolved oxygen consumption caused by the decay of dead phytoplankton (Fig,11b). These results worked together to decrease the bottom dissolved oxygen and create hypoxic expansion (Fig.11c). Scully (2013) illustrated how changes in wind associated with stratification and thereby hypoxia on the shelf. They found that increased wind speed decreased the hypoxic area, whereas decreased wind speed facilitated hypoxia development. These findings were consistent with our results.

Changes in wind direction also significantly influence the hypoxic area off Yangtze Estuary. As seen in Fig. 12a, when the mean summer wind direction was from north (W180^{o}), stratification was decreased in the north of 31^{o}N and along the coast of Zhejiang relative to the Base model run. This would lead to an enhancement of vertical dissolved oxygen flux. Whereas near to the Hangzhou bay, the vertical dissolved oxygen flux was reduced

associated with increased water stratification, resulting in decreased bottom dissolved oxygen (Fig. 12c).Under the control of the northerly wind (W180^o), Yellow coastal current was enhanced, bringing the high dissolved oxygen from the north of Yellow Sea to the Yangtze Estuary. This further led to increased bottom dissolved oxygen off Yangtze Estuary. From the Fig. 12b, it can be seen that surface chlorophyll concentration in the W180^o was lower than the Base model run. We attributed this to the fact that wind from the north drive downwelling due to Ekman dynamics. Decreased dissolved oxygen consumption was caused by the reduced decay of dead phytoplankton. When the summer wind was from the East (W-90^o), the average water stratification was similar to the W180^o wind run, but the integrated hypoxic area in W-90^o wind run was larger than the W180^o. This may be related to the horizontal distribution of chlorophyll concentration. As shown in Fig. 12b, surface chlorophyll concentration was higher in W-90^o wind run than the W180^o run, which would lead to more dissolved oxygen consumption caused by organic matter decomposition in W-90^o. When the summer wind was from the west (W+90^o), stratification was the strongest in the three wind direction runs. And integrated hypoxic area also reached the maximum. There can be three reasons. For the first reason, Fig. 12a showed that stratification was stronger in the most areas, except in the north of the 31.5^{o}N relative to the Base model run, which suggested that in most areas the water mixing was week and the vertical flux of dissolved oxygen reduced. For the second reason, under the influence of the westerly wind, the residual flow would transport the low dissolved oxygen from the trough off the Yangtze Estuary to the eastward. For the third reason, from Fig. 12b, it can be found an area of relatively high chlorophyll concentration off Yangtze Estuary in W+90^o wind run. This may be due to Yangtze River which was rich in nutrients expand to the eastward under the controlling of westerly wind. As a result, it would promote the growth of phytoplankton. The decomposition of dead phytoplankton was another important factor for the decreased bottom dissolved oxygen. These reasons work together to create hypoxic conditions.

5. Conclusions

In this study, a three-dimensional coupled physical-biological model was used to analyze the hypoxia off to the Yangtze Estuary. This study highlighted that river discharge, wind speed and wind direction all had significant impacts on the hypoxia. The seasonal cycle of hypoxia was relatively insensitive to the temporal variability in river discharge. But the integrated hypoxic area was very sensitive to the magnitude of river discharge. Increasing in the magnitude of river discharge led to enhance stratification, promote the growth of phytoplankton associated with higher nutrients, and thereby greatly increased hypoxic area off the Yangtze Estuary. In contrast, decreased in the magnitude of river discharge reduced the stratification and surface chlorophyll concentration and hence

significantly decreased the hypoxic area.

Model simulations demonstrated that wind speed and wind direction not only play an important role in the seasonal cycle of hypoxia, but also in the integrated the hypoxic area. When the winds in January were repeated all year, the hypoxic zone was nearly disappeared as the result of the strong water mixing induced by strong, northerly winds. While persistently weak winds from August enhanced stratification and facilitated hypoxia development. Increasing wind speed weakened stratification and chlorophyll-a concentration, hence decreased the hypoxic area, while decreasing wind speed did the opposite. Wind direction significantly influenced the extent of hypoxia. Among the directions runs, the integrated hypoxic area was greatest when the summer wind came from the west (W + 90^{o}), which was enhanced by nearly 20%. When the summer wind direction was from the north (W180^{o}), the integrated hypoxic area off Yangtze Estuary was minimum. The integrated hypoxic area reduced by nearly 10% when the wind was from the east (W-90^{o}).

The model did not include inorganic phosphorus and therefore assumed that primary production was limited by light and nitrogen only. In future studies, the model needs to consider the dynamics of inorganic phosphorus. In addition, increasing the number of monitoring cruises per year and setting up additional long-term moorings in the East China Sea would be useful to further validate biogeochemical variables and environmental factors.

References

Chapman, D. C.: Numerical treatment of cross-shelf open boundaries in a barotropic coastal ocean model, Journal of Physical oceanography, 15, 1060-1075, 1985.

Chen, J., Ni, X., Liu, M., Chen, J., Mao, Z., Jin, H., and Pan, D.: Monitoring the occurrence of seasonal low-oxygen events off the Changjiang Estuary through integration of remote sensing, buoy observations, and modeling, Journal of Geophysical Research: Oceans, 119, 5311-5322, 10.1002/2014jc010333, 2014.

Diaz, R. J.: Overview of hypoxia around the world, J Environ Qual, 30, 275-281, 2001.

Feng, Y., Fennel, K., Jackson, G. A., DiMarco, S. F., and Hetland, R. D.: A model study of the response of hypoxia to upwelling-favorable wind on the northern Gulf of Mexico shelf, Journal of Marine Systems, 131, 63-73, 10.1016/j.jmarsys.2013.11.009, 2014.

Fennel, K., Hu, J., Laurent, A., Marta-Almeida, M., and Hetland, R.: Sensitivity of hypoxia predictions for the northern Gulf of Mexico to sediment oxygen consumption and model nesting, Journal of Geophysical Research: Oceans, 118, 990-1002, 10.1002/jgrc.20077, 2013.

Flather, R.: A tidal model of the northwest European continental shelf, Mem. Soc. Roy. Sci. Liege, Ser. 6, 10, 141-164, 1976.

Goni, M., Gordon, E., Monacci, N., Clinton, R., Gisewhite, R., Allison, M., and Kineke, G.: The effect of Hurricane Lili on the distribution of organic matter along the inner Louisiana shelf (Gulf of Mexico, USA), Continental Shelf Research, 26, 2260-2280, 10.1016/j.csr.2006.07.017, 2006.

Gu, H.: The maximum value of dissolved oxygen in its vertical distribution in Yellow SEA, Acta Oceanologica Sinica, 1980.

Haidvogel, D. B., Arango, H., Budgell, W. P., Cornuelle, B. D., Curchitser, E., Di Lorenzo, E., Fennel, K., Geyer, W. R., Hermann, A. J., and Lanerolle, L.: Ocean forecasting in terrain-following coordinates: Formulation and skill assessment of the Regional Ocean Modeling System, Journal of Computational Physics, 227, 3595-3624, 2008.

Karlson, K., Rosenberg, R., Bonsdorff, E., Gibson, R., Barnes, M., and Atkinson, R.: Temporal and spatial large-scale effects of eutrophication and oxygen deficiency on benthic fauna in Scandinavian and Baltic waters - A review, Oceanography and Marine Biology, Vol 40, 40, 427-489, 2002.

Katja Fennel, J. W., Julia Levin, John Moisan: Nitrogen cycling in the Middle Atlantic Bight: Results from a three-dimensional model and implications for the North Atlantic nitrogen budget, GLOBAL BIOGEOCHEMICAL CYCLES, 20, GB3007, 2006.

Lewis, M. R., Cullen, J. J., and Platt, T.: Phytoplankton and thermal structure in the upper ocean: consequences of nonuniformity in chlorophyll profile, Journal of Geophysical Research: Oceans (1978–2012), 88, 2565-2570, 1983.

Li, H., Chen, J., Lu, Y., Jin, H., Wang, K., and Zhang, H.: Seasonal variation of DO and formation mechanism of bottom water hypoxia of Changjiang River Estuary, Journal of Marine Sciences, 29, 78-87, 2011.

Liu, K.-K., Chao, S.-Y., Lee, H.-J., Gong, G.-C., and Teng, Y.-C.: Seasonal variation of primary productivity in the East China Sea: A numerical study based on coupled physical-biogeochemical model, Deep Sea Research Part II: Topical Studies in Oceanography, 57, 1762-1782, 10.1016/j.dsr2.2010.04.003, 2010.

Liu Xincheng, S. H., Huang Qinghui: Concentration variation and flux estimation of dissolved inorganic nutrient from the Changjiang River, Chinese Journal of Oceanology and Limnology, 33, 332-340, 2002.

Liu Zhiguo, X. R., Liu Caicai,Qin Yutao,Cai Peng: Characters of hypoxia area off the Yangtze River EStuary and its influence, Marine science bulletin, 31, 588-593, 2012.

Marchesiello, P., McWilliams, J. C., and Shchepetkin, A.: Open boundary conditions for long-term integration of regional oceanic models, Ocean modelling, 3, 1-20, 2001.

Mellor G , T. Y.: Development of a turbulence closure model for geophysical fluid problems, Geophys, 20, 851-875, 1982.

Morel, A., and Berthon, J. F.: Surface pigments, algal biomass profiles, and potential production of the euphotic layer: Relationships reinvestigated in view of remote‐sensing applications, Limnology and Oceanography, 34, 1545-1562, 1989.

Murphy, R. R., Kemp, W. M., and Ball, W. P.: Long-Term Trends in Chesapeake Bay Seasonal Hypoxia, Stratification, and Nutrient Loading, Estuaries & Coasts, 34, 1293-1309, 2011.

Ni, X., Huang, D., Zeng, D., Zhang, T., Li, H., and Chen, J.: The impact of wind mixing on the variation of bottom dissolved oxygen off the Changjiang Estuary during summer, Journal of Marine Systems, 2014.

Ning, X., Lin, C., Su, J., Liu, C., Hao, Q., and Le, F.: Long-term changes of dissolved oxygen, hypoxia, and the responses of the ecosystems in the East China Sea from 1975 to 1995, Journal of Oceanography, 67, 59-75, 2011.

Obenour, D. R., A. Michalak, and D. Scavia: Assessing biophysical controls on Gulf of Mexico hypoxia through probabilistic modeling, Ecological Applications, 25, 492-505, 2015.

Rabouille, C., Conley, D. J., Dai, M. H., Cai, W. J., Chen, C. T. A., Lansard, B., Green, R., Yin, K., Harrison, P. J., Dagg, M., and McKee, B.: Comparison of hypoxia among four river-dominated ocean margins: The Changjiang (Yangtze),

Mississippi, Pearl, and Rhône rivers, Continental Shelf Research, 28, 1527-1537, 10.1016/j.csr.2008.01.020, 2008.

Scully, M. E.: Wind Modulation of Dissolved Oxygen in Chesapeake Bay, Estuaries and Coasts: J ERF, 33, 1164-1175, 10.1007/s12237-010-9319-9, 2010a.

Scully, M. E.: The Importance of Climate Variability to Wind-Driven Modulation of Hypoxia in Chesapeake Bay, Journal of Physical Oceanography, 40, 1435-1440, 10.1175/2010jpo4321.1, 2010b.

Scully, M. E.: Physical controls on hypoxia in Chesapeake Bay: A numerical modeling study, Journal of Geophysical Research: Oceans, 118, 1239-1256, 10.1002/jgrc.20138, 2013.

Shchepetkin A F, M. J. C.: The regional oceanic modeling system(ROMS): a split—explicit, free—surface, topography-following-coordinate oceanic model, Ocean Modelling, 9, 347-404, 2005.

Vaquer-Sunyer, R., and Duarte, C.: Thresholds of hypoxia for marine biodiversity, Proceedings of the National Academy of Sciences of the United States of America, 105, 15452-15457, 10.1073/pnas.0803833105, 2008.

Wang, B.: Hydromorphological mechanisms leading to hypoxia off the Changjiang estuary, Marine Environmental Research, 67, 53-58, 10.1016/j.marenvres.2008.11.001, 2009.

Wei, H., He, Y., Li, Q., Liu, Z., and Wang, H.: Summer hypoxia adjacent to the Changjiang Estuary, Journal of Marine Systems, 67, 292-303, 10.1016/j.jmarsys.2006.04.014, 2007.

Wei, Q., Wang, B., Chen, J., Xia, C., Qu, D., and Xie, L.: Recognition on the forming-vanishing process and underlying mechanisms of the hypoxia off the Yangtze River estuary, Science China Earth Sciences, 58, 628-648, 2015.

Wilson, R. E., Swanson, R. L., and Crowley, H. A.: Perspectives on long-term variations in hypoxic conditions in western Long Island Sound, Journal of Geophysical Research, 113, 10.1029/2007jc004693, 2008.

Wiseman, W. J., Rabalais, N. N., Turner, R. E., Dinnel, S. P., and Macnaughton, A.: Seasonal and interannual variability within the Louisiana coastal current: stratification and hypoxia, Journal of Marine Systems, volume 12, 237-248, 1997.

X Li, Z. Y., X Song, X Cao: The seasonal characteristics of dissolved oxygen distribution and hypoxia in the Changjiang Estuary, Journal of Coastal Research, 27, 2011.

Xia, M., and Jiang, L.: Influence of wind and river discharge on the hypoxia in a shallow bay, Ocean Dynamics, 65, 665-678, 10.1007/s10236-015-0826-x, 2015.

Yin, K., Lin, Z., and Ke, Z.: Temporal and spatial distribution of dissolved oxygen in the Pearl River Estuary and adjacent coastal waters, Continental Shelf Research, 24, 1935–1948, 2004.

Zhou F, H. D., Ni X: Hydrographic analysis on the multi-time scale variability on hypoxia adjacent to the Changjiang River estuary, Acta Ecol Sin, 30, 4728-4720, 2010.

Zhu, Z.-Y., Zhang, J., Wu, Y., Zhang, Y.-Y., Lin, J., and Liu, S.-M.: Hypoxia off the Changjiang (Yangtze River) Estuary: Oxygen depletion and organic matter decomposition, Marine Chemistry, 125, 108-116, 10.1016/j.marchem.2011.03.005, 2011.

458
459
460
461
462
463
464
465
466
467
468
469
470
471
472
473
474
475
476
477
478
479
480
481
482
483
484
485
486
487
488
489
490
491
492
493
494
495
496
497
498
499
500
501
502
503
504

带格式的：缩进：首行缩进： 0 字符

Table.1 Model sensitivity experiment

Experiments	Description
Base model run	
Base	Base run with realistic river discharge and wind forcing in year 2010
River discharge runs	
Qconst	River discharge was set to annual average value
Q2	Double the river discharge
Q0.5	Halve the river discharge
Wind runs	
WJan	Winds from January were repeated for every month of the year
WAug	Winds from August were repeated for every month of the year
W0.9	Summer (July–September) wind magnitude was decreased by 10%
W1.1	Summer (July–September) wind magnitude was increased by 10%
W180°	Summer (July–September) wind direction was rotated 180°
W-90°	Summer (July–September) wind direction was rotated negative 90°
W+90°	Summer (July–September) wind direction was rotated positive 90°

Table.2 The total area of hypoxia area under different thresholds of DO, and the average N^2 in summer and the year

Experiments	Integrated Hypoxic Area (10^3 km^2 days)			Average N^2	
	<1mg/L	<2mg/L	<3mg/L	Summer average	Yearly average
Base model run					
Base	11.7	330.5	1163	5.58×10^{-4}	2.63×10^{-4}
River runs					
Qconst	8.0 (- 32%)	179.6 (- 46%)	939.3 (- 19%)	3.80×10^{-4} (-32%)	2.24×10^{-4} (-15%)
Q2	94.1(+704%)	634.8(+92%)	1640.4(+41%)	10×10^{-4} (+79%)	5.03×10^{-4} (+91%)
Q0.5	4.33 (- 63%)	147.1 (- 55%)	927.7 (- 20%)	3.28×10^{-4} (-41%)	1.59×10^{-4} (-40%)
Wind runs					
WJan	0 (-100%)	13.9 (-96%)	256.8 (- 78%)	4.06×10^{-4} (- 27%)	1.90×10^{-4} (-28%)
WAug	25.4(+117%)	412.8 (+25%)	1435.3(+23%)	6.25×10^{-4} (+12%)	3.02×10^{-4} (+15%)
W0.9	49.0(+319%)	478.0 (+45%)	1296.8(+12%)	6.29×10^{-4} (+13%)	2.80×10^{-4} (+6%)
W1.1	0 (-100%)	118.9 (- 64%)	894.4 (- 23%)	4.89×10^{-4} (- 12%)	2.45×10^{-4} (- 7%)
W180°	13.8 (+18%)	235.5 (- 29%)	909.4 (- 22%)	4.97×10^{-4} (-11%)	2.45×10^{-4} (- 7%)
W-90°	14.6 (+25%)	296 (- 10%)	1020.5(-12%)	5.07×10^{-4} (- 9%)	2.51×10^{-4} (- 5%)
W+90°	20.3 (+74%)	390.9 (+18%)	1240 (+7%)	6.68×10^{-4} (+20%)	2.85×10^{-4} (+8%)

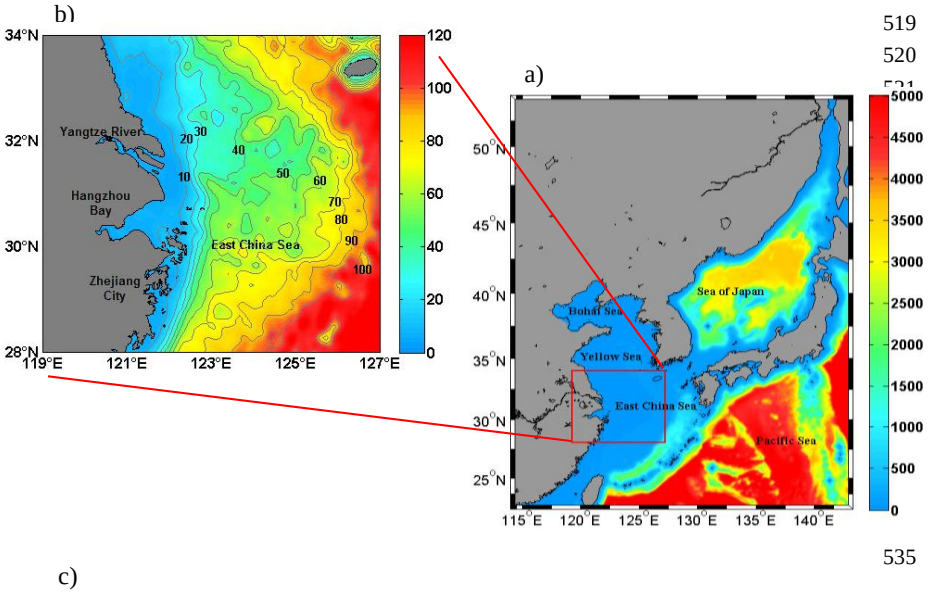

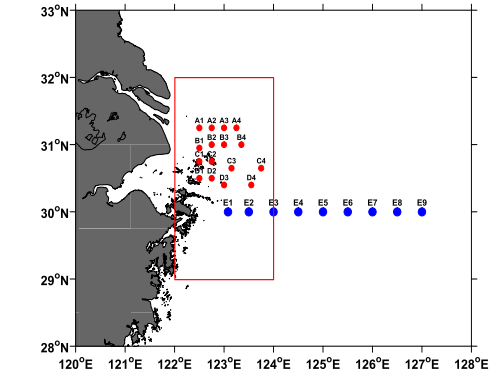

Fig.1 (a) Model domian and depth. Red box is the region of Fig.1b. (b) The model bathymetry (shading map, unit: meter) of East China Sea. (c) Red dots are the station observation in August 2011, blue dots are the section observation in August 2011, the red rectangle indicates the region used for the calculation of N^2.

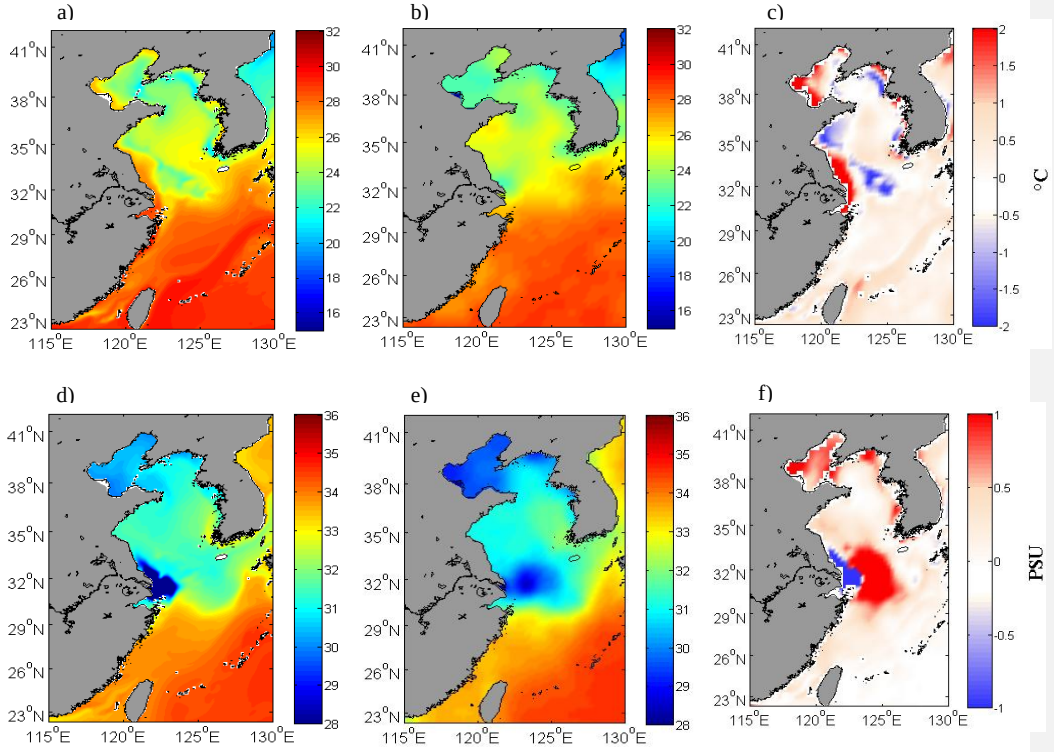

Fig.2 The comparison between modeled results (a) and GDEM data (b) of climatological field of SST in August, and the difference between them (c). The comparison between modeled results (d) and GDEM data (e) of climatological field of SSS in August, and the difference between them (f).

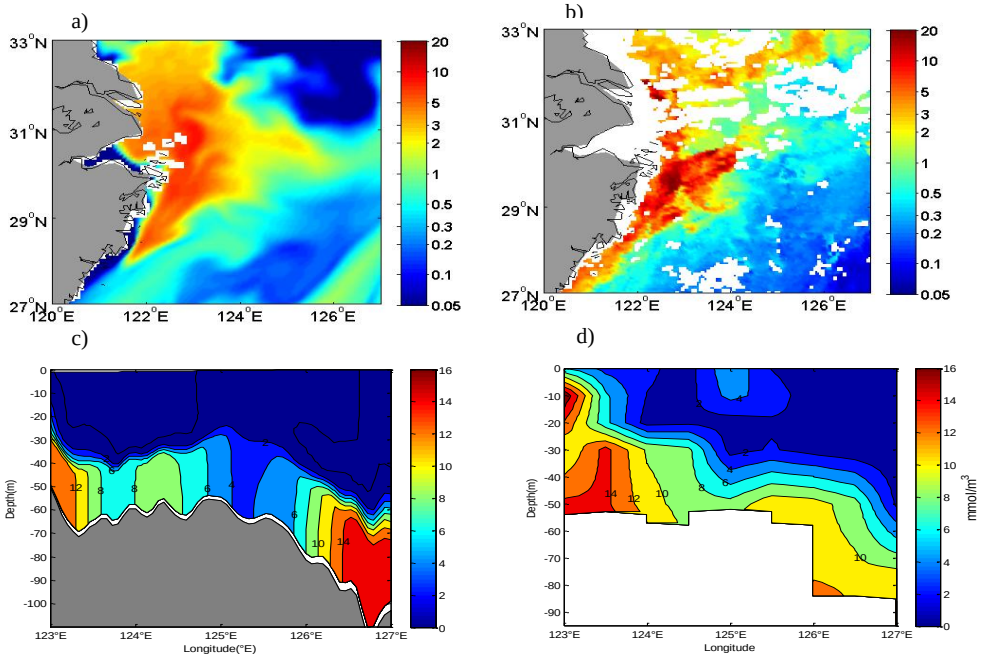

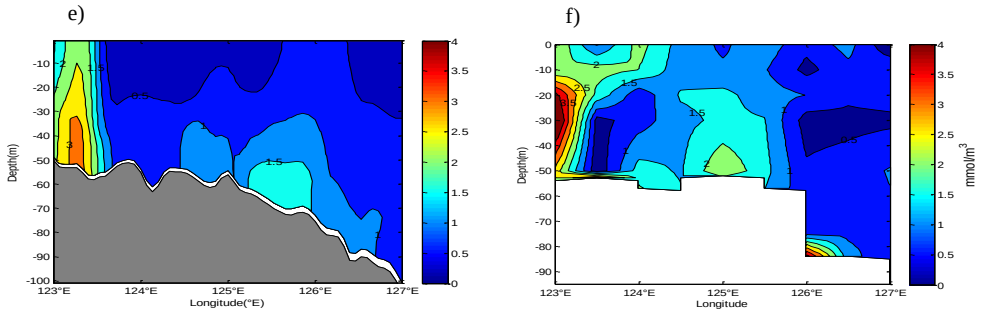

Fig.3 The comparison between modeled results (a) and MODISA~~SeaWiFS~~-derived data (b) of chlorophyll-a concentration in August 201~~0~~. The comparison between modeled results (c) and in-situ data (d) of NO_3 along the section of 30°N in August 2011. The comparison between modeled results (e) and in-situ data (f) of NH_4 along the section of 30°N in August 2011.

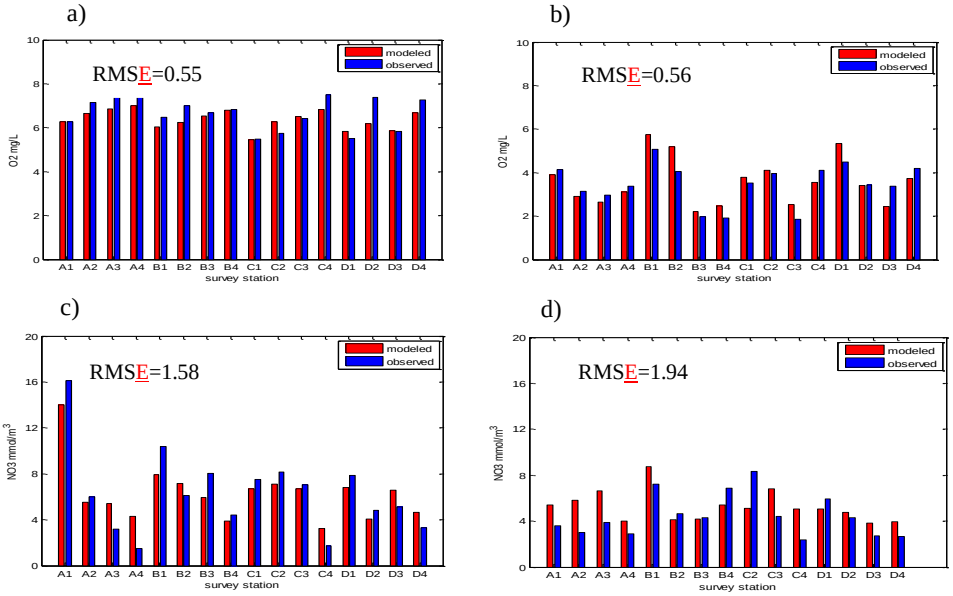

Fig.4 The comparison between modeled results (red bars) and observed data (blue bars) of NO_3 and DO at the stations in August 2011 (see Figure 1c). (a), (b) Respectively represent the surface DO and bottom DO; (c), (d) Respectively, represent the surface NO_3 concentration and bottom NO_3 concentration

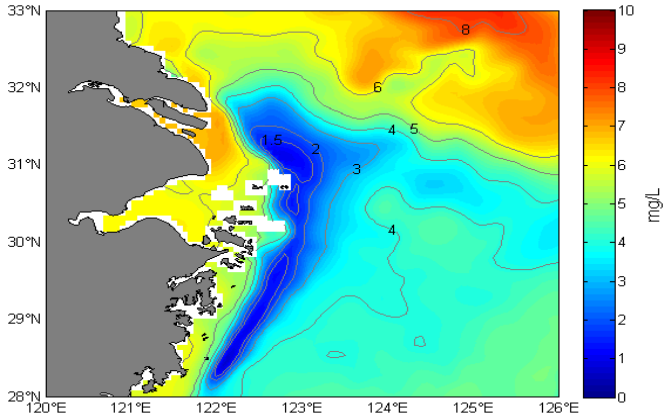

Fig.5 The modeled patterns of hypoxia zone off the Yangtze Estuary in September 2010

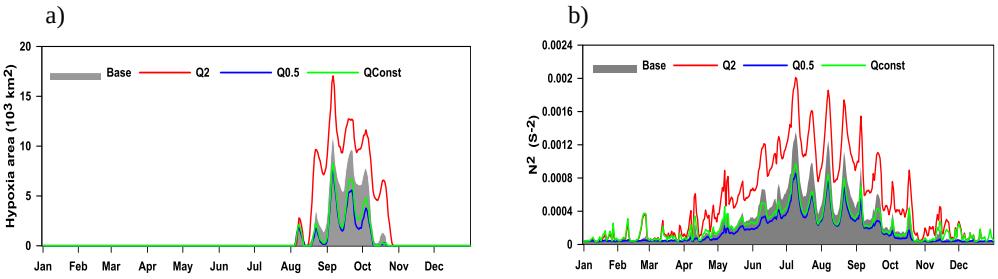

Fig.6 (a), (b) are the hypoxia area (DO<2mg/L) and N^2 in the river discharge experiment, respectively. The gray shaded part represents the Base run and the red, blue, green curve represent Q2, Q0.5, Qconst, respectively.

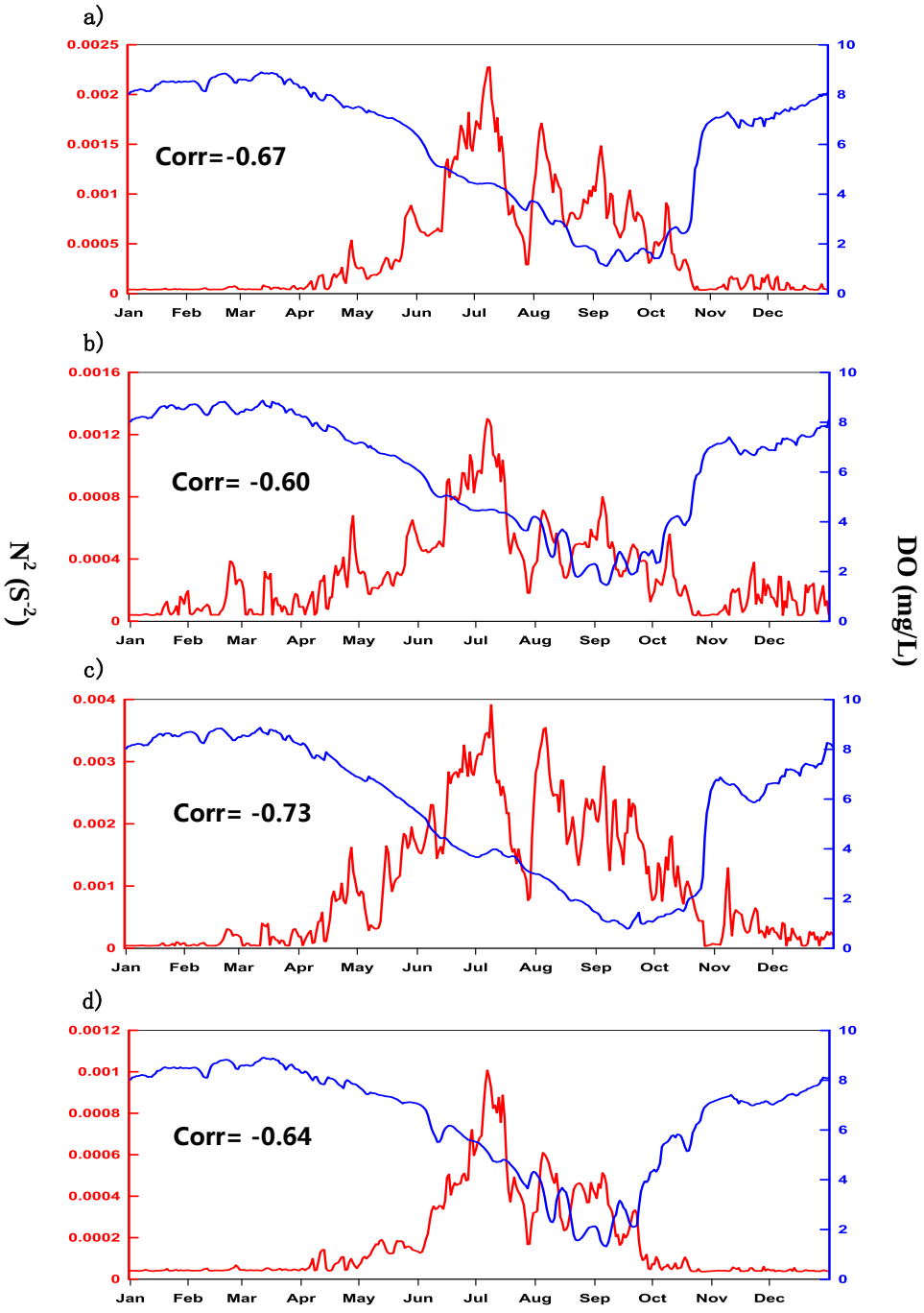

Fig.7 The correlation between the bottom dissolved oxygen concentration and N^2 in the station of 123°E, 31°N. The blue curve represents the bottom dissolved oxygen concentration, and the red curve represents N^2. (a), (b), (c), (d) respectively represent the Base run, Qconst, Q2, Q0.5.

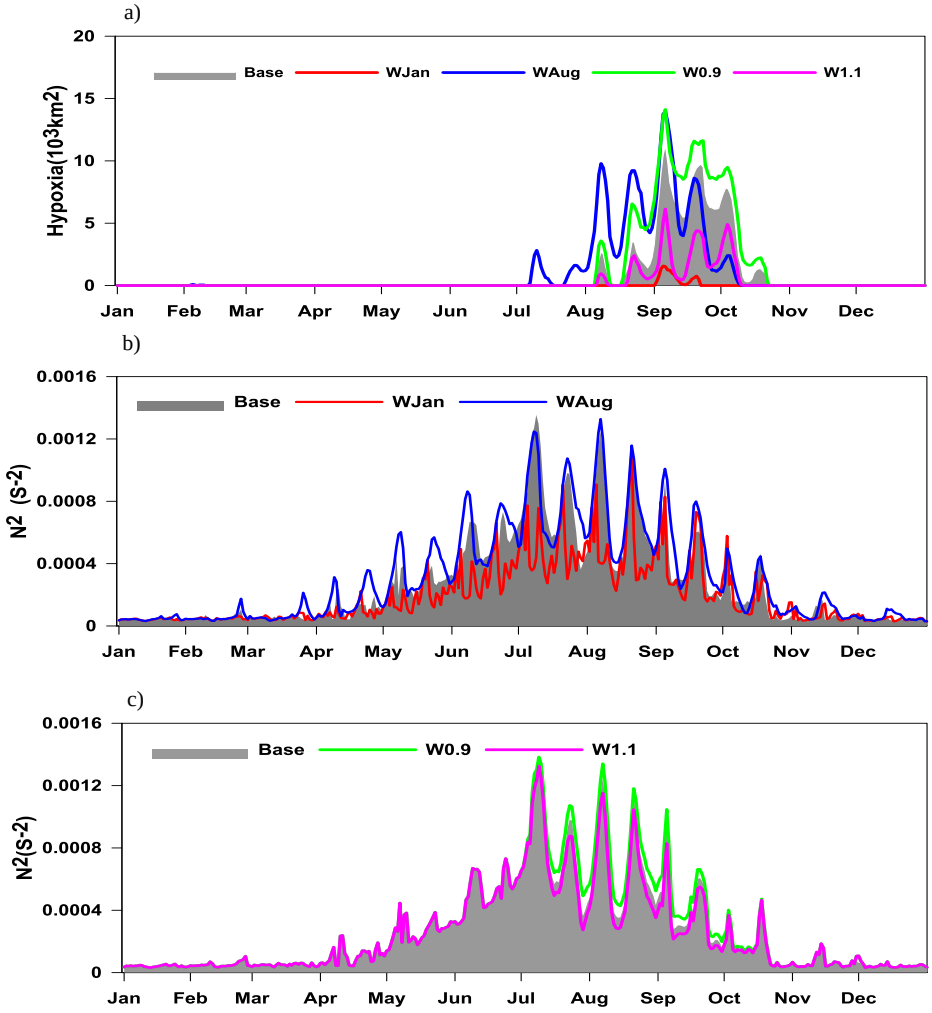

Fig.8 (a) The comparison of the simulated hypoxic area (DO<2mg/L) on the wind variation runs. (b),(c) Averaged stratification N2 for the Base run (gray shadow) and wind variation runs

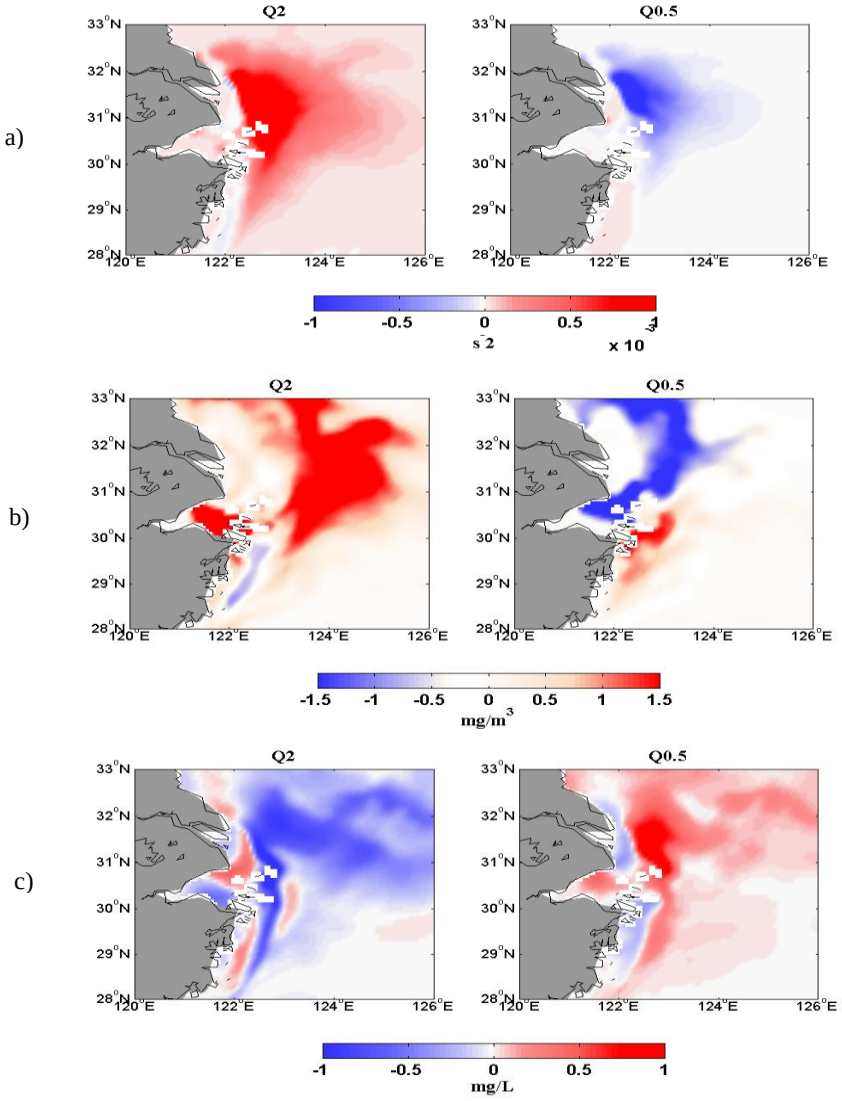

Fig.9 (a) The deviation in summer (7-9 months) stratification(N^2) of Q2, Q0.5 from the Base run. (b)The deviation in summer (7-9 months) chlorophyll concentration of Q2, Q0.5 from the Base run. (c) The deviation in summer (7-9 months) bottom dissolved oxygen concentration of Q2, Q0.5 from the Base run.

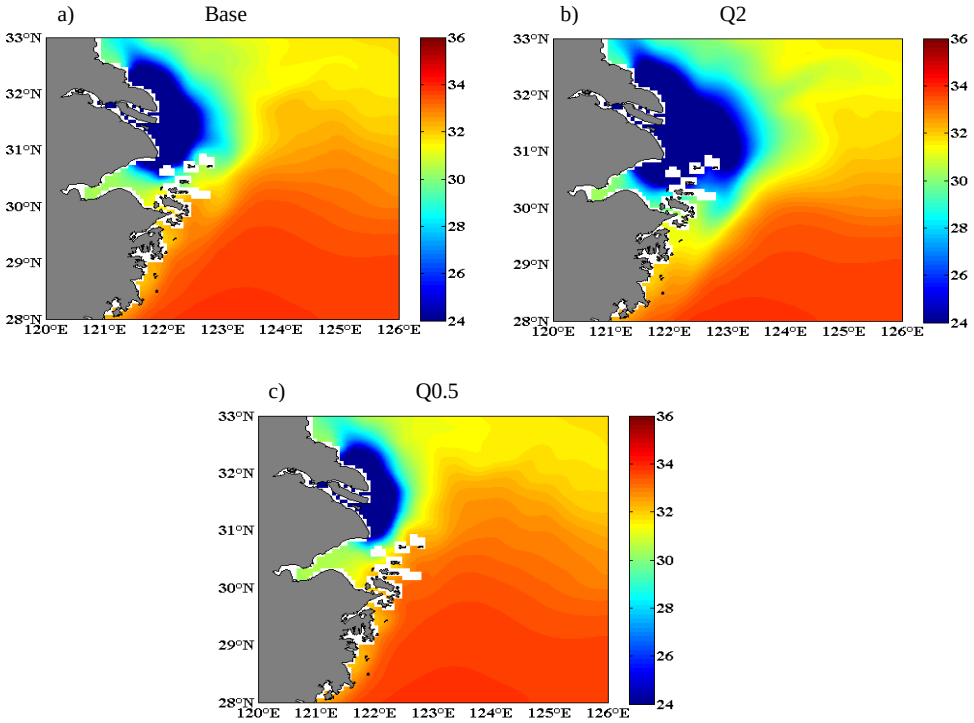

Fig.10 Averaged surface salinity for the period July to September in 2010 for the river runs. (a), (b), (c) respectively represent the Base run, Q2, Q0.5.

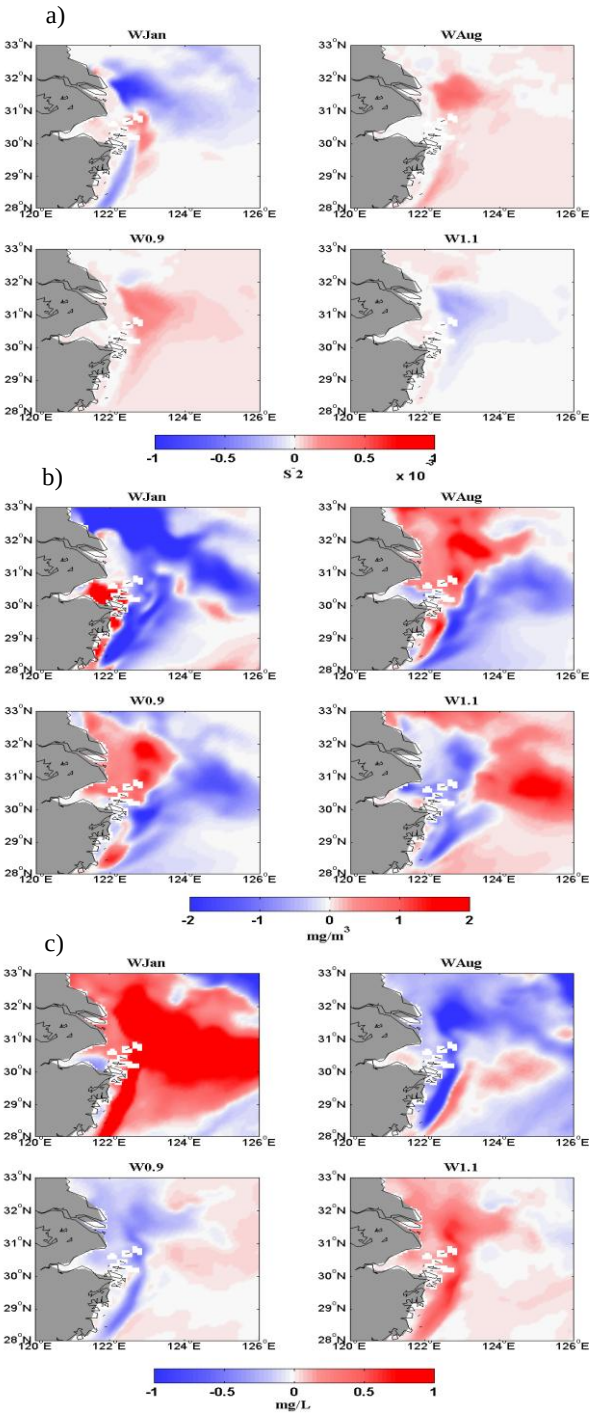

Fig.11 (a) The deviation in summer (7-9 months) stratification(N^2) of wind variation runs from the Base model. (b) The deviation in summer (7-9 months) chlorophyll concentration of wind variation runs from the Base model. (c) The deviation in summer (7-9 months) bottom dissolved oxygen concentration of wind variation runs from the Base model

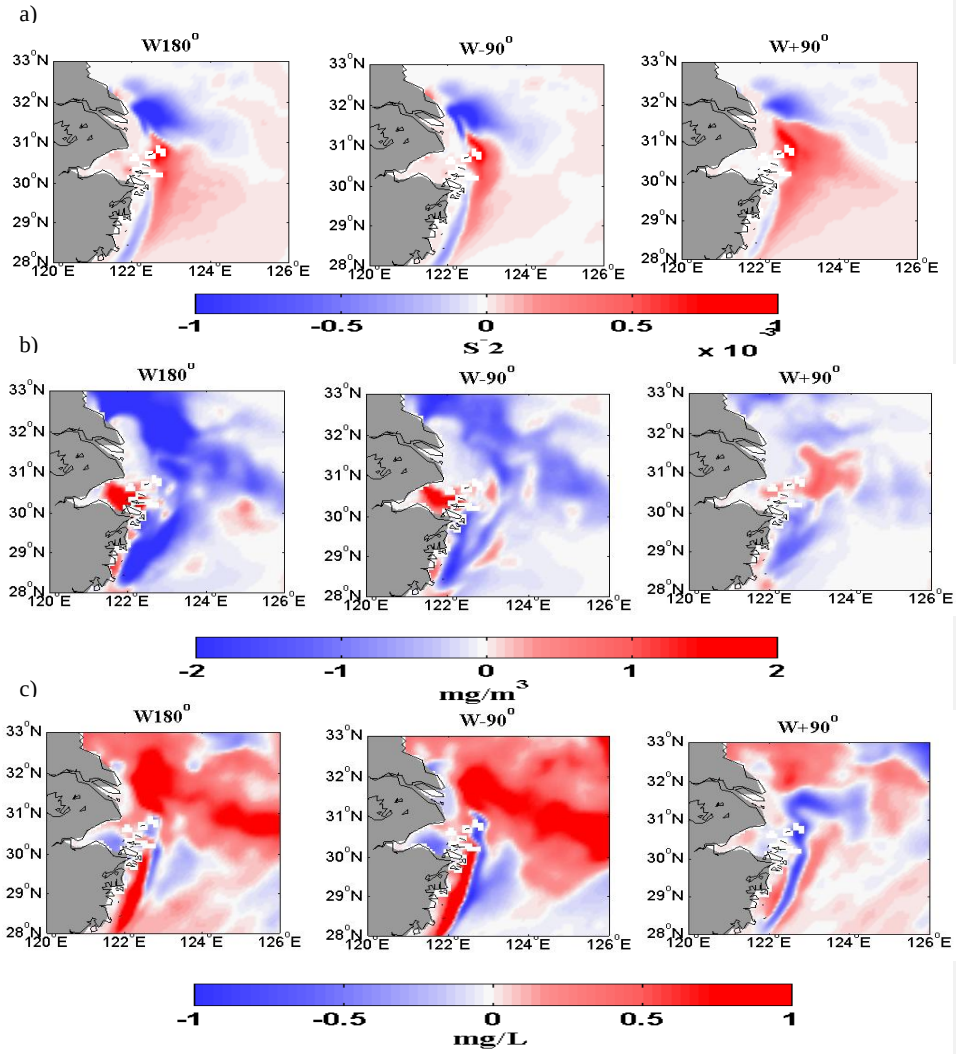

Fig.12 (a) The deviation in summer (7-9 months) stratification(N^2) of wind direction variation runs from the Base model. (b) The deviation in summer (7-9 months) chlorophyll concentration of wind direction variation runs from the Base model. (c) The deviation in summer (7-9 months) bottom dissolved oxygen concentration of wind direction variation runs from the Base model